

A Convergent Dynamic Window Approach to Obstacle Avoidance

Petter Ögren, *Member, IEEE*, and Naomi Ehrich Leonard, *Senior Member, IEEE*

Abstract—The dynamic window approach (DWA) is a well-known navigation scheme developed by Fox *et al.* and extended by Brock and Khatib. It is safe by construction, and has been shown to perform very efficiently in experimental setups. However, one can construct examples where the proposed scheme fails to attain the goal configuration. What has been lacking is a theoretical treatment of the algorithm's convergence properties. Here we present such a treatment by merging the ideas of the DWA with the convergent, but less performance-oriented, scheme suggested by Rimon and Koditschek. Viewing the DWA as a model predictive control (MPC) method and using the control Lyapunov function (CLF) framework of Rimon and Koditschek, we draw inspiration from an MPC/CLF framework put forth by Primbs to propose a version of the DWA that is tractable and convergent.

Index Terms—Lyapunov function, mobile robots, model predictive control (MPC), navigation function (NF), obstacle avoidance, receding horizon control (RHC), robot control.

I. INTRODUCTION

THE PROBLEM of robotic motion planning is a well-studied one, see, for instance, [10]. One of the early approaches is artificial potential fields, where the robot is driven by the negative gradient of a sum of potentials from different obstacles and the goal. Many of these methods suffer from the problem of undesired local minima, i.e., positions different from the goal, where the robot could get stuck. The most refined method along these lines is perhaps [4], where advanced mathematics is applied to construct an artificial potential function without undesired local minima. Other approaches have used ideas from fluid mechanics or electro magnetics [18], [19] to construct functions free of local minima, but they are, in general, computationally intensive and therefore ill-suited for dynamic environments.

There is also a direction of research toward biologically motivated, nonmodel-based methods. These include fuzzy or neural

Manuscript received February 19, 2003; revised October 23, 2003. This paper was recommended for publication by Associate Editor Y. Liu and Editor S. Hutchinson upon evaluation of the reviewers' comments. The work of P. Ögren was supported by the Swedish Foundation for Strategic Research through its Center for Autonomous Systems at the Royal Institute of Technology, Stockholm, Sweden. The work of N. E. Leonard was supported in part by the Office of Naval Research under Grants N00014-98-1-0649 and N00014-01-1-0526, in part by the National Science Foundation under Grant CCR-9980058, and in part by the Air Force Office of Scientific Research under Grant F49620-01-1-0382. This paper was presented in part at the IFAC World Congress, Barcelona, Spain, July 2002, and in part at IEEE IROS, Lausanne, Switzerland, October 2002.

P. Ögren is with the Department of Autonomous Systems, Swedish Defense Research Institute, SE-172 90 Stockholm, Sweden (e-mail: petter.ogren@foi.se).

N. E. Leonard is with the Mechanical and Aerospace Engineering Department, Princeton University, Princeton, NJ 08544 USA (e-mail: naomi@princeton.edu).

Digital Object Identifier 10.1109/TRO.2004.838008

approaches and the behavior-based paradigm described in, e.g., [12]. A recent attempt to incorporate mathematical formalism into such frameworks can be seen in [8], but they are still, in general, hard to analyze from a convergence perspective. In cluttered environments, the exact shape of the robot must be taken into account; these aspects have been investigated in [13] and [16]. Most work, however, as well as our study, assume a circular or point-shaped robot.

We build our proposed scheme on the combination of a model-based optimization scheme and a convergence-oriented potential field method. A large class of model-based techniques use optimization to choose from a set of possible trajectories [1], [2], [14], [15]. We argue that these optimization-based techniques can be seen as applications of a model predictive control (MPC) approach (or, equivalently, a receding horizon control (RHC) approach). Having made this observation, we look at the method of exact robot navigation using artificial potential functions, put forth by Rimon and Koditschek [4]. After constructing a continuously differentiable navigation function (NF) (artificial potential), Rimon and Koditschek use Lyapunov theory to prove convergence. Bounded control and safety is shown, but the method has the drawback of almost never using the full control authority, and furthermore, is not suited for dynamic environments where fast response to changes is essential. Inspired by Primbs *et al.* [3], we present a way to merge the convergent Koditschek scheme with the fast reactive dynamic window approach (DWA). This is done by casting the two approaches in an MPC and control Lyapunov function (CLF) framework, respectively, and combining the two as suggested by Primbs *et al.* The conceptual flowchart of this combination is depicted in Fig. 1.

The organization of this paper is as follows. In Section II, we review the work of [1] and [2], as well as [3]. Then, we explain our proposed scheme in detail in Section III. In Section IV, we discuss the theoretical properties of our approach, and in Section V, we give a simulation example. The conclusions can be found in Section VI. This paper builds on our earlier work [5], [6].

II. PREVIOUS WORK USED IN THIS PAPER

In this section, we discuss the ideas of Fig. 1 in some detail.

A. The DWA and Its Extension

The DWA [1] is an obstacle-avoidance method that takes into account the dynamic and kinematic constraints of a mobile robot (many of the vector field and vector field histogram approaches do not). The basic scheme involves finding the *admissible controls*, those that allow the robot to stop before hitting an obstacle

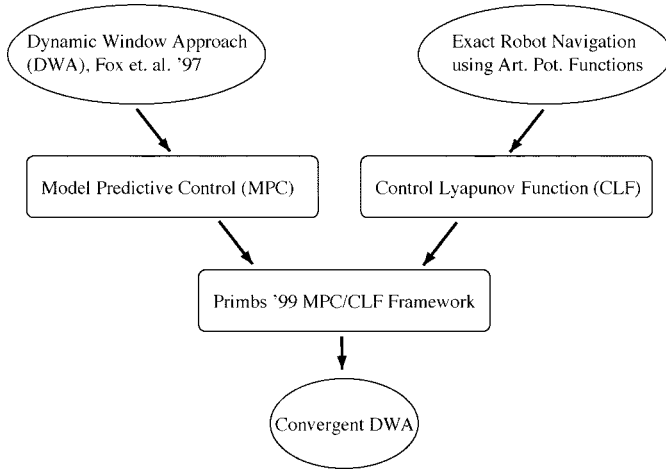


Fig. 1. Idea of the proposed approach can be seen as combining elements from the original DWA with a construction guaranteeing convergence, proposed by Rimon and Koditschek. This is done with inspiration from an MPC/CLF framework suggested by Primbs *et al.*

while respecting the above constraints. Then an optimization is performed over those admissible controls to find the one that gives the highest utility in some prescribed sense. There are different suggestions for the utility function in [1] and [2], including components of velocity alignment with preferred direction, large minimum clearances to obstacles, possibility to stop at the goal point, and the norm of the resulting velocity vector (large being good).

Brock *et al.* [2] extended the work in [1] by looking at holonomic robots (Fox *et al.* considered synchro-drive ones), and more importantly, by adding information about connectivity to the goal. The latter was done by replacing the goal-direction term with the negative gradient of an NF , defined as the length of the shortest (unobstructed) path to the goal [10]. Thus, they were able to eliminate the local minima problems present in so many obstacle-avoidance schemes (hence, the term “Global” in the title of [2]).

The experimental results reported in [1] and [2] are excellent, showing consistent safe performance at speeds up to 1.0 m/s with a Nomadic Technologies XR4000 robot [2]. The results demonstrate an algorithm that is safe by construction (in the sense that the robot never hits obstacles), and displays high efficiency in extensive experimental tests. But although Brock and Khatib argue that the use of an NF makes the approach “Global,” it is never formally shown. In fact, examples can be constructed where the robot enters a limit cycle, never reaching the goal, or actually consistently moving away from the goal (see Section III-D).

B. Exact Robot Navigation Using Artificial Potential Fields

One of the main contributions of [4] is the clever construction of a special artificial potential. This potential has no local minima except the global minimum at the goal. Furthermore, it is continuously differentiable and attains its maximum value at all the obstacle boundaries.

Combining such a potential $NF(r)$, where $r \in \mathbb{R}^2$ is position, with a kinetic energy term, one can construct a CLF as

$$V(r, \dot{r}) = \frac{1}{2} \dot{r}^T \dot{r} + NF(r).$$

TABLE I
COMPLEMENTARY PROPERTIES OF THE TWO APPROACHES

CLF	MPC
Global information	Local information
Stability oriented	Performance oriented
Off-line analysis	On-line computation
Hamilton Jacobi Bellman type	Euler-Lagrange type

The dynamics $\ddot{r} = u$ and the control $u = -\nabla NF + d(r, \dot{r})$, where $d(r, \dot{r})$ is a dissipative force, yields $\dot{V} \leq 0$ and stability in the Lyapunov sense (see the Appendix for definitions of stability and Lyapunov function).

The controls are bounded, since ∇NF is continuous on a compact set. Further, the fact that $\dot{V} \leq 0$ and $NF(r) = NF_{\max}$ at the obstacle boundaries guarantees against collisions if the initial velocity is small enough. The construction is, however, only valid in *a priori* known “generalized sphere worlds” containing obstacles of specific categories. To adjust the scheme to a specific robot requires a scaling of NF to make the maximal $\nabla NF(r)$ smaller than the robot control bound. This, in turn, will make the vast majority of prescribed control signals far below the bound, resulting in very slow progress toward the goal.

We draw inspiration from the work in [4]; however, we relax the constraints on ∇NF from continuous to piecewise-continuous and remove the requirement that $NF(r) = NF_{\max}$ at the boundaries. By doing this, we hope to gain computational efficiency in calculating (and recalculating in case of new information) the NF , and also to allow quite general obstacle shapes. Furthermore, removing these constraints gives the possibility of adding the constraint $\|\nabla NF(r)\| = c$ (where c is a scalar constant) used to enhance performance by allowing the consistent use of control signals close to the given bound.

C. CLFs and MPC

In an interesting paper by Primbs *et al.* [3], the connection between CLFs and MPC is investigated (MPC is also known as RHC). They note the complementary properties shown in Table I. In view of these properties, they suggest the following framework to combine the complementary advantages of each approach. The control law is chosen to satisfy a short-horizon optimal control problem under constraints that ensure the existence of a CLF. The problem becomes one of finding a control u and a CLF $V(x)$ that satisfy (1)–(4) as follows

$$u = \arg \inf_{u(\cdot)} \int_t^{t+T} (q(x) + u^T u) d\tau \quad (1)$$

$$\text{subject to } \dot{x} = f(x) + g(x)u \quad (2)$$

$$\frac{\partial V}{\partial x} (f + gu) \leq -\epsilon \sigma(x(t)) \quad (3)$$

$$V(x(t+T)) \leq V(x_\sigma(t+T)) \quad (4)$$

where $q(x)$ is a cost on states, $\epsilon > 0$ is a scalar, $T > 0$ is the horizon length, $\sigma(x)$ is a positive definite function, and x_σ is the trajectory when applying a pointwise minimum norm control scheme (for details, see [3]). This formulation inspires our choice of a more formal, continuous-time formulation of the DWA, allowing us to prove convergence.

III. A PROVEN CONVERGENT DWA

In the main parts of this paper, we will use the notation $x = (r, \dot{r}) = (r_x, r_y, \dot{r}_x, \dot{r}_y)$ for the state of the system. We adopt the robot model from [2], which is basically a double integrator in the plane $\dot{r} = u$, $r \in \mathbb{R}^2$ with bounds on the control $\|u\| \leq u_{\max}$, and on the velocity $\|\dot{r}\| \leq v_{\max}$. Note that it was shown in [9] that an off-axis point on the unicycle robot model described by

$$\begin{aligned}\dot{r}_x &= v \cos \theta \\ \dot{r}_y &= v \sin \theta \\ \dot{\theta} &= \omega \\ \dot{v} &= \frac{F}{m} \\ \dot{\omega} &= \frac{\tau}{J}\end{aligned}$$

can be feedback linearized to $\dot{r} = u$.

For the environment, we assume that the robot's sensors can supply an occupancy grid map, i.e., a rectangular mesh with each block being marked as either free or occupied, over the immediate surroundings. Here, the size of the robot must be taken into account, and additional safety margins, due to, e.g., localization errors, can be added. For example, if localization errors are bounded, the obstacle regions can be expanded by the corresponding amount, so that performance of the algorithm described below will still be guaranteed. A position marked as free means that the robot does not intersect any obstacles when occupying that position. Thus, a map can be incrementally built as the robot moves around. We assume, as did Brock and Khatib, that the simultaneous localization and mapping (SLAM) problem (see, e.g., [21]) is solved for us.

In cases where we are given a probabilistic occupancy grid, a heuristic weighting in the utility function (10) is conceivable. Other methods use a graph with weighted edge costs, reflecting ease of traversal. Such ideas are, however, not applicable to this scheme, due to the nature of the proof of *Lemma 3.1*.

A. Navigation Function

In our setting, the navigation function $\text{NF}(r)$, [2], [4], [10] approximately maps every free space position to the length of the shortest collision-free path going from that position to the goal point. Note that the details of our version are slightly different from both [2] and [4], since the former is only piecewise-constant, while the latter has to be at least C^2 . To be more precise, we make the following definition.

Definition 3.1 (NF): By an NF, we mean a continuous function defined on the connected part of the obstacle-free space $\subset \mathbb{R}^2$, containing the goal point and mapping to the real numbers. An NF has only one local minimum, which is also the global minimum. The set of local maxima is of measure zero. ∇NF is piecewise-continuous, and the projection of the left and right limits along the discontinuity edges satisfy $e^T \nabla_{\text{left}} \text{NF}(r) = e^T \nabla_{\text{right}} \text{NF}(r)$, where $e \in \mathbb{R}^2$ is the direction of the edge and $\nabla_{\text{left(right)}} \text{NF}(r)$ is the gradient on each side of it.

Before investigating how to construct such a function in detail, we note that it is shown in [2] how to deal with the case when the robot at first only knows its immediate surroundings

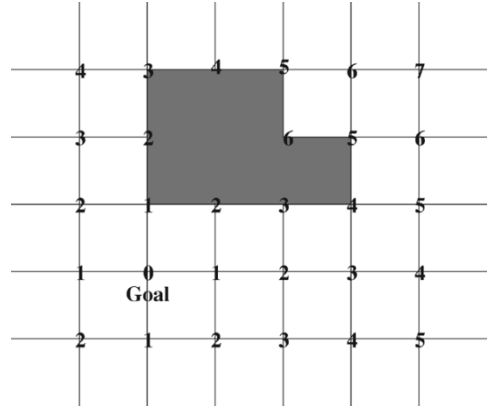


Fig. 2. Graph discretization and computed shortest-path distances. Shaded squares correspond to an obstacle.

by use of its sensors. The idea is to assume free space at the unknown positions, and then recalculate the NF when sensor data showing the opposite arrives. In this way, the robot guesses good paths and updates them when new information arrives. The information is immediately taken into account in the optimization [see (10)], thus avoiding collisions. The less urgent recalculation of the NF is then done. These updates are made at a time scale much slower than the actual motion control, so in our considerations below, we assume the map to be static. Brock and Khatib [2] used the gradient of the NF as the desired heading, instead of using just the goal direction, as Fox did [1].

To compute the NF, we will use a technique similar to the one suggested in [2]. There, however, the NF was piecewise-constant in the grids; here, we need a local-minima-free continuous function defined on all free space, making things somewhat more complicated. The basic idea is to solve the shortest-path problem in a graph discretization, and then make a careful continuous interpolation for the positions in between the discretization points. An example of the discretization can be seen in Fig. 2. We note that while the grid is four-directional, the resulting robot velocities are not constrained to these directions; indeed, the robot will often descend the gradient of the NF by traversing the grids diagonally.

Lemma 3.1 (Construction of NF): An NF can be created by the following procedure.

- 1) Make a graph out of the rectangular mesh of the obstacle grid map, with vertices at the corners of each square and edges along the square edges. Remove vertices and edges that are in the interior of obstacles.
- 2) One of the vertices is chosen as goal point.
- 3) Solve the shortest-path problem in the graph (can be done with polynomial time algorithms [11]). Mark each vertex with the corresponding path length, and let this length be the value of the NF at the vertex.
- 4) Divide the squares into triangles by drawing a diagonal through the corner with the highest NF value (this is shown to be unique later).
- 5) In the interior of each resulting triangle, let $\text{NF}(r)$ be a linear interpolation between NF at the three vertices, i.e., let the value of $\text{NF}(r)$ be a plane intersecting the three vertices.

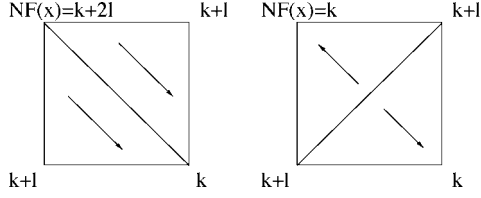


Fig. 3. Two possible cases, unique lowest $NF(x)$ (left, as in the square northwest of the goal point in Fig. 2) and two equal (right, as in the square northeast of the obstacle in Fig. 2). The arrows indicate $-\nabla NF$.

Proof: We begin by showing that there are no local minima on the graph vertices and edges. Note that for a given pair of vertices (A, B) , if one path between A and B has even (odd) length (in multiples of the edge length l), so has any other path. Therefore, two neighbors cannot have the same NF value. Since $NF(r)$ on the edges is a linear interpolation between the value on the vertices, the edges have no local minima. Furthermore, from every vertex, there is a shortest path to goal, and along this path, NF decreases monotonically. Thus, there can be no local minimum vertex, except the goal point.

Now we look at the values in the interior of the squares. Given a square, look at the corner of lowest value, which may or may not be unique. If it is unique and of value k , then the two adjacent corners must have value $k+l$, where l is the side length, and the opposite corner must have $k+2l$, since no adjacent corners have the same value (see Fig. 3, left). The diagonal is from $k+2l$ to k , and in this case, the two triangles will actually form an inclined plane, which obviously has no interior local minimum.

If the lowest value is not unique, the opposite corner must have the same value k and the two adjacent ones, $k+l$ (see Fig. 3, right). The diagonal is between the two $k+l$ corners (unique as stated in the construction), and this diagonal composes a ridge of local maxima. There are, however, no local minima.

Thus, we have seen that there is only one local minimum, the goal point. There might be local maxima on some diagonals, as in Fig. 3 (right), but they are isolated lines, and thus, of measure zero. Finally, since NF is composed of triangles glued together, the projection along the edges fulfills $e^T \nabla_{\text{left}} NF(r) = e^T \nabla_{\text{right}} NF(r)$ as above. ■

With an NF at our disposal, we are ready to look at the actual choice of control.

B. General Control Scheme

The basic idea for the convergence proof is the same as in [4]. First, we write the problem as a conservative system with an artificial potential, and then we introduce a dissipative control term. This dissipative control term is the sum of a turning force (gyroscopic term) and a braking force (strictly dissipative term). Chang and Marsden also identify a gyroscopic-plus-dissipative control term for obstacle avoidance [20]. In the conservative system, we choose the artificial potential to be $(k/\sqrt{2})NF(r)$, where k is a positive constant that must be chosen smaller than the control bound u_{\max} . Otherwise, the set C_2 , defined later, will be empty, as seen in Fig. 4. The CLF is

$$V(x) = \frac{1}{2} \dot{r}^T \dot{r} + \frac{k}{\sqrt{2}} NF(r) \quad (5)$$

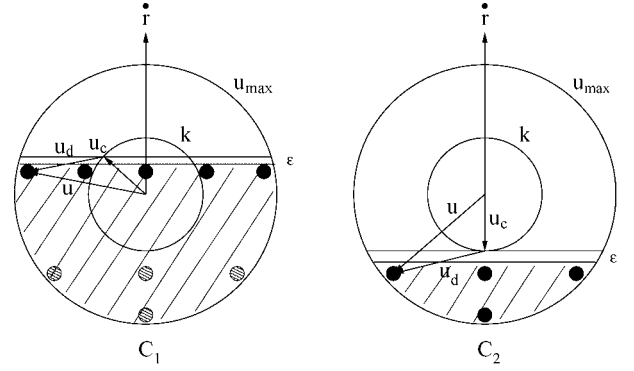


Fig. 4. Control sets C_1 and C_2 .

where $NF(r)$ is the NF as explained above. Incorporating the upper bounds on the control magnitude, we define the dissipative control set as follows.

Definition 3.2 (Dissipative Controls, $C_d(r, \dot{r})$):

$$C_d(r, \dot{r}) = \left\{ u : u = u_c + u_d, u_c = -\frac{k}{\sqrt{2}} \nabla NF \right. \\ \left. u_d : u_d^T \dot{r} < -\epsilon \|\dot{r}\| < 0, \text{ if } \dot{r} \neq 0, \|u\| \leq u_{\max} \right\}$$

for some given $\epsilon > 0$. We write $u \in C_d(r, \dot{r})$.

A typical shape of the $C_d(r, \dot{r})$ set is the shaded regions in Fig. 4, where C_1 (the nine dots) is a discretized (finite) subset of C_d . Note that $\|u_c\| = \|(k/\sqrt{2})\nabla NF(r)\| = k$, since $\|\nabla NF(r)\| = \sqrt{2}$, (the directional derivative along each axis of the grid is equal to one, the gradient direction is diagonal to the grid, and the magnitude is $\sqrt{1^2 + 1^2}$, see Fig. 3). Thus u_c lies on a circle of radius k . The outer circle of radius u_{\max} bounds the control set.

Now the problem is to make sure the robot does not run into obstacles. In the standard DWA, this is taken care of by choosing among *admissible*, i.e., not colliding, controls in an optimization. Here we shall do the same.

A general formulation of the combined CLF/MPC scheme now looks like this

$$u = \arg \min_{u(\cdot)} V(x(t+T)) \quad (6)$$

$$\text{subject to } u(s) \in C_d(r, \dot{r}) \quad \forall s \in [t, t+T] \quad (7)$$

$$r(s) \text{ collision free } \forall s \in [t, t+T] \quad (8)$$

$$\dot{r}(t+T) = 0 \quad (9)$$

where T is the horizon length of the MPC. Here (7) gives stability in the Lyapunov sense. Safety is guaranteed by (8) and (9), i.e., a planned collision-free trajectory ending with the robot standing still. This corresponds to the policy of driving a car slow enough so that you can always stop in the visible part of the road. This is perhaps somewhat conservative on a highway, but sensible on a small forest road where fallen trees might block your way.

Note that the above formulation can, in principle, be applied to enhance the performance of any approach with an artificial potential having a well-behaved gradient, e.g., the original NF suggested in [4] or a version of [18] and [19]. We believe that the

NF suggested above is a choice that yields high robot velocities and good computational efficiency.

The optimal control problem of the MPC above can be computationally intensive, as seen in related approaches, such as [7]. Therefore, we devote the next section to showing how a very coarse discretization can still yield quite good performance. In Section IV, we give detailed proofs of the theoretical properties of the proposed method.

C. Discretized Control Scheme

To end up with a computationally tractable version of the MPC, we discretize the set of dissipative controls C_d into two sets with piecewise-constant controls, relative to the velocity direction. The horizon length is $T = T_1 + T_2$, where T_1 is the time over which the resulting control will be applied. After time T_1 , a new optimization is performed. The control set C_d is discretized into two sets, C_1 and C_2 , corresponding to the two time intervals of length T_1 and T_2 . A third set C_s is used when starting from a standstill, see *Definition 3.3*. To make the scheme precise, we formulate the following algorithm.

Algorithm 3.1 (Control Scheme): The control algorithm is composed of the following steps, where step 3 is the main one.

- 1) If $\dot{r} = 0$, choose the control pair $(C_s, C_{2\text{middle}})$, as given in *Definition 3.3*, i.e., start out in a good direction.
- 2) Else, if $t \geq t_0 + T_{\text{timeout}}$, then set the new $t_0 = t$. If furthermore, $V(t_0) - V(t) \leq \Delta V_{\text{timeout}}$, then take the C_2 part $C_{2\text{prev}}$ of the previous control pair and choose the control pair $(C_{2\text{prev}}, C_{2\text{prev}})$, i.e., reset and stop safely.
- 3) Else, choose the optimal solution to the MPC control problem

$$\begin{aligned} & \min_{C_1 \times C_2} V(x(t+T)) \\ & \text{subject to } x(\cdot) \text{ is collision-free.} \end{aligned} \quad (10)$$

- 4) Apply the first part of the chosen control pair for T_1 time units, then repeat from 1.

Here, $\Delta V_{\text{timeout}}$ is a user-defined decrease in V over the time T_{timeout} . This timeout construction is needed to guarantee against the hypothetical case of the robot velocity slowly approaching zero. Then the decrease bound $\dot{V} \leq \epsilon \|\dot{r}\|$ is not enough to yield convergence. The control sets are defined as follows.

Definition 3.3 (Control Sets, C_1 , C_2 , and C_s): Let C_1 be the set of nine controls depicted as solid and shaded dots in Fig. 4, left, and C_2 be the set of four controls (a subset of C_1) in Fig. 4, right. Note that C_1 and C_2 are defined relative to the velocity direction \dot{r} . Furthermore, let C_s be the control directed toward the corner of the current grid with the lowest NF(r) value (if there are more than one such corner, the one closest to the robot is chosen) and with control magnitude such that after applying C_s for time T_1 , and the middle, hardest braking control of C_2 for time T_2 , the robot stops at the corner.

Intuitively, the scheme can be visualized as a downhill skier on the slopes of the NF. Then the set of controls in $C_1 \setminus C_2$ correspond to using all the acceleration provided by the slope while possibly turning (gyroscopic forces). The set $C_1 \cap C_2$, on the other hand, corresponds to maximal braking maneuvers

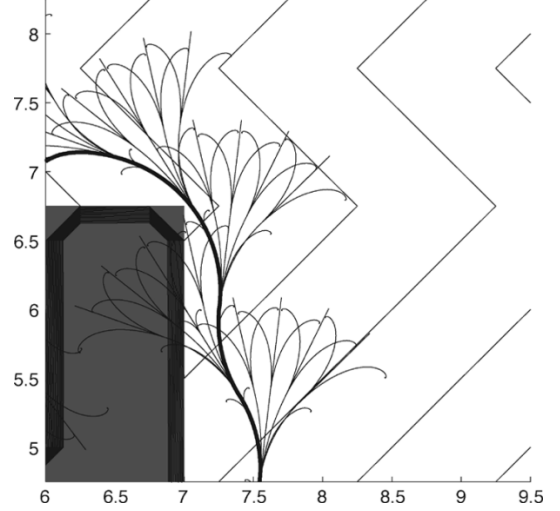


Fig. 5. An obstacle, level curves of the NF, and parts of a trajectory, as well as all the considered options.

(dissipative forces). The coarseness of the discretization, i.e., the cardinality of the sets C_1 and C_2 , can be varied with respect to the amount of computational resources available.

As seen in Fig. 4, choosing k close to the upper bound u_{max} makes the set C_2 cover a very small area, while choosing k small limits the maximal forward acceleration available to the vehicle.

Note that $C_s \subset C_d$, since the acceleration is toward the corner closest to goal. We further assume the grids to be small enough to be traversable by the $C_s \times C_2$ control in $T_1 + T_2$ time units. To make the current grid unique, positions on the boundary of grids are assigned to belong to one of the adjacent grids.

The interval $[t, t+T]$ is divided into two parts, $[t, t+T_1]$ and $[t+T_1, t+T]$, where T_1 is the time step of the MPC control loop. In the first part $[t, t+T_1]$, a control from C_1 , the set of controls in Fig. 4, left, is chosen. In the second part $[t+T_1, t+T]$, a control from C_2 , the set of controls in Fig. 4, right, is chosen. Note that the controls in the sets above are constant with respect to the direction of the robot velocity, \dot{r} . C_2 consists of four controls (the dots in Fig. 4, right) all reducing the speed of the robot. C_1 consists of five controls on the border of the dissipative region (shaded area) and the four C_2 controls (the shaded dots). Thus, the whole set $C_1 \times C_2$ consists of $(5 + 4) \cdot 4 = 36$ control sequences.

In Fig. 5, we see parts of an executed trajectory together with all the options evaluated in the optimization. An obstacle, as well as the level curves of the NF, are also depicted.

It can be seen that in the first time step, the leftmost control of C_1 is chosen, and in the second time step, the rightmost control is chosen. Since T_1 is the length of the time step, it is only the C_1 part of $C_1 \times C_2$ that is actually executed.

The purpose of the C_2 part is to guarantee safety. The time $T = T_1 + T_2$ should be chosen long enough for the robot to stop at (or before) time $t+T$ (since all the C_2 controls are braking). The optimization is done with the constraint that the resulting trajectory does not hit any obstacles, hence, the choice of the rightmost control the second time. The fact that the previously chosen C_2 control is an option in C_1 makes the last part of the (safe) previously chosen control sequence an option in the next

optimization. As a result, there is always at least one admissible (and therefore, safe) control sequence available. As stated above, this is similar to always making sure you can stop in the visible part of the road when driving a car.

One might argue that discretization and exhaustive search is an inelegant solution. But we chose it for two reasons. The utility function $V(x(t+T))$ varies rather slowly over the admissible set of controls, and this set, in turn, can be very complex, e.g., unconnected if there are traversable paths to the right and to the left, but the road straight ahead is blocked by an obstacle. The constraints are also far from being a differentiable function inequality. Due to these facts, a steepest-descent approach will not do well.

D. Example of Convergence Failure of Previous Approach

The utility function of [2] that is to be maximized is

$$\Omega_g(p, v, a) = \alpha \cdot n f 1(p, v) + \beta \cdot \text{vel}(v) + \gamma \cdot \text{goal}(p, v) + \delta \cdot \Delta n f 1(p, v, a)$$

where p, v, a are the current position, desired velocity, and acceleration, respectively. $\alpha, \beta, \gamma,$ and δ are scalar weights, $n f 1(p, v)$ increases if the velocity is aligned with the NF gradient, $\text{vel}(v)$ increases with velocity (if far from goal), $\text{goal}(p, v)$ is binary, 1 if the trajectory will pass through the goal point, and $\Delta n f 1$ is the decrease in NF value.

Consider a ‘‘T’’-shaped, very narrow corridor, with the robot initially in the top left end and the goal defined in the bottom end. This will leave the robot accelerating maximally toward the right. If the corridor is long and narrow enough, the speed is going to be too great to allow a right turn at the intersection. Thus, the robot will continue away from the goal. In particular, when the corridor is very narrow and turning is not an option, the robot must either brake or not. If the weights are such that the velocity term $\text{vel}(v)$ outweighs the $\Delta n f 1$ term, the robot will just keep on going. Otherwise, it will brake maximally. If, however, the acceleration is as powerful as the retardation, the robot will oscillate back and forth in the upper part of the ‘‘T,’’ and never be able to make the sharp turn into the goal part of it. A similar counterexample was independently presented in [7]. Note that the Lyapunov property of (11) removes these kinds of problems in the proposed approach.

IV. PROOF OF CONVERGENCE AND SAFETY

Before we formulate the main theorem of this paper we need a lemma.

Lemma 4.1 (CLF): The function

$$V(x) = \frac{1}{2} \dot{r}^T \dot{r} + \frac{k}{\sqrt{2}} \text{NF}(r)$$

is a CLF, and any C_d control satisfies the following inequality:

$$\dot{V}(x) \leq -\epsilon \|\dot{r}\|. \quad (11)$$

Proof: The candidate CLF is $V(x) = (1/2)\dot{r}^T \dot{r} + (k/\sqrt{2})\text{NF}(r)$, which is clearly positive definite with a global minimum at $x_{\text{goal}} = (r_{\text{goal}}, 0)$. Differentiating with respect to time gives $\dot{V}(x) = \dot{r}^T u + (k/\sqrt{2})\dot{r}^T \nabla \text{NF}(r) = \dot{r}^T (u_c + u_d + (k/\sqrt{2})\nabla \text{NF}(r)) \leq -\epsilon \|\dot{r}\|$, by the constraints on u . The NF

is, however, not differentiable everywhere. Along the triangle edges of NF, there are, in general, two different (left and right) limits of the gradient. The projections along the edge is the same, $\dot{r}^T \nabla_{\text{left}} \text{NF}(r) = \dot{r}^T \nabla_{\text{right}} \text{NF}(r)$, making the inequality true. Furthermore, it is this projection that is needed when determining u according to the definition of u_d ; see *Definition 3.2* and Fig. 4.

If \dot{r} is not parallel to an edge, the problem with undefined $\nabla \text{NF}(r)$ in the control will only occur in one isolated time instant, and thus, $\int \dot{V} dt$ is not changed by whatever value we use. ■

Theorem 4.1 (Finite Completion Time): Suppose the control scheme in *Algorithm 3.1* is used, and there is a traversable path from start to goal in the occupancy grid. Then, the robot will reach the goal position in a time bounded above by

$$T_{\text{goal}} \leq \left(V_0 \frac{\sqrt{2} 1}{k l} 2 \right)^2 (T_{\text{timeout}} + T_1 + T_2) + \frac{V_0}{\Delta V_{\text{timeout}}} T_{\text{timeout}}$$

where $V_0 = V(x_{\text{start}})$ is the value of the CLF at the starting position.

Proof: By *Lemma 4.1*, we have that $\dot{V}(x) \leq -\epsilon \|\dot{r}\|$. Thus, the system is stable in the sense of Lyapunov.

After a stop, the robot starts moving toward the corner of the current grid closest to goal, i.e., with lowest $\text{NF}(r)$. Then, the optimization improves on this, making the outcome at least as good as stopping at that corner (at a stop, $V(r, \dot{r} = 0) = (k/\sqrt{2})\text{NF}(r)$). Together with the fact that $\dot{V}(x) \leq 0$, this means that the robot will never stop in that grid again. Thus, the number of possible grids to occupy (which is finite) is reduced by at least one between each pair of stops. Since NF is the path length, the number of possible grids is bounded by $(V_0(\sqrt{2}/k)(1/l)2)^2$. Therefore, this is also a bound on the number of stops. The timeout induces a stop if $V(t_0) - V(t_0 + T_{\text{timeout}}) \leq \Delta V_{\text{timeout}}$. This makes the number of T_{timeout} -sized intervals without a stop bounded by $V_0/\Delta V_{\text{timeout}}$. Combining the two, we get $T_{\text{goal}} \leq (V_0(\sqrt{2}/k)(1/l)2)^2 (T_{\text{timeout}} + T_1 + T_2) + (V_0)/(\Delta V_{\text{timeout}}) T_{\text{timeout}}$. ■

Remark 4.1: Note that this is an extreme worst-case analysis. In the simulations, the robot did not stop at all before reaching the goal position.

Theorem 4.2 (Safety): Suppose the control scheme in *Algorithm 3.1* is used, and the robot starts at rest in an unoccupied position. Then, the robot will not run into an obstacle.

Proof: The proof relies on the recursive structure of $C_1 \times C_2$. The subset of noncolliding controls in $C_1 \times C_2$ (that we are optimizing over) is never empty, since we can always choose the C_2 (not yet applied) part of the previous $C_1 \times C_2$ control sequence as our new C_1 control. ■

V. SIMULATION EXAMPLE

To illustrate the approach, we chose a setting with three large obstacles in a 9×9 m area, as seen in Fig. 6. We used parameters for the Nomadic Technologies XR4000 robot obtained from [2], $\|u\| \leq u_{\text{max}} = 1.5$ m/s², $\|\dot{r}\| \leq v_{\text{max}} = 1.2$ m/s. We furthermore set the parameters as follows: $T_1 = 0.5$ s, $T_2 = 2$ s,

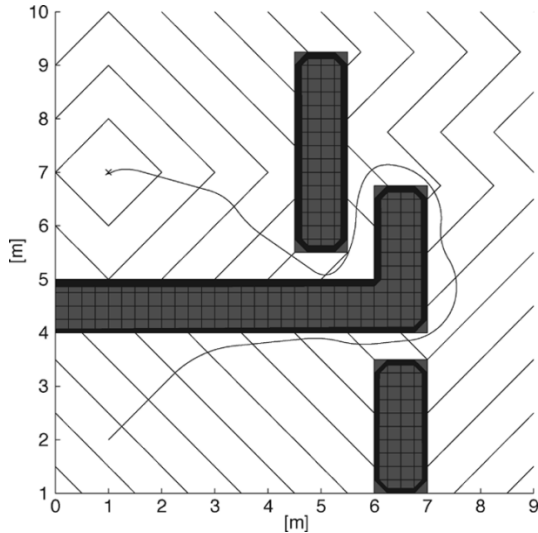


Fig. 6. Obstacles and robot trajectory.

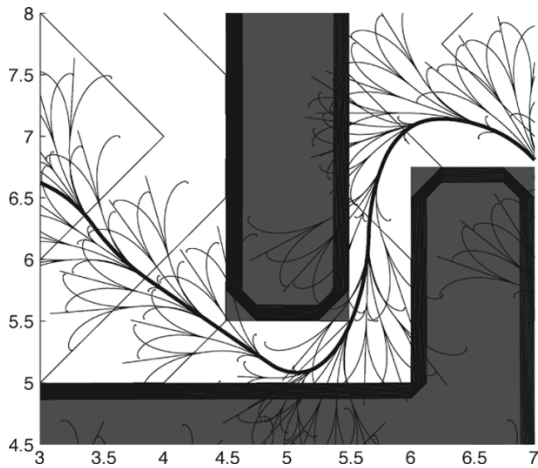


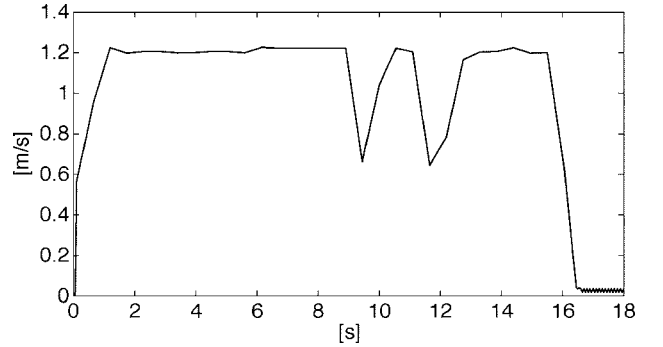
Fig. 7. Closeup of parts of the trajectory including all the evaluated options of the MPC. The robot slows down in two places, (6.5,7.2) and (5.5,5.5), in order not to collide.

$k = 1/\sqrt{2}$. The resulting robot trajectory and the level curves of the NF are also depicted in the figure. Note the absence of local minima as guaranteed by the construction in *Lemma 3.1*. In the beginning and the end of the trajectory, it can be seen how the MPC minimization in (10) favors going perpendicular to the level curves.

In Fig. 7, parts of the trajectory as well as the MPC options are shown. The robot slows down in two places, as can be seen in Fig. 8. These are located at (6.5,7.2) and (5.5,5.5), respectively. In the second instance, all the nonbraking C_1 controls make the robot collide. The sharp-braking right turn, the C_2 part of the previous choice, is, however, safe and therefore applied. At the first instance, (6.5,7.2), the nonbraking right turn is safe, but the braking left turn yields a lower $V(x(t+T))$ value (it is closer to the goal) and is thus chosen.

To enforce the $\|\dot{r}\| \leq v_{\max} = 1.2$ m/s bound, we impose the additional acceleration constraint

$$u^T \dot{r} \frac{1}{\|\dot{r}\|} \leq \frac{v_{\max} - \|\dot{r}\|}{T_1}.$$

Fig. 8. Robot velocity. Note how the speed is limited by $v_{\max} = 1.2$ m/s and how it decreases twice during the narrow passage.

This constraint is of the same sort as the dissipative constraint, i.e., it can be depicted as another horizontal line above or below the ones in Fig. 4. If the new constraint is more restrictive (lies below the first two), the C_1 options will be placed just below it, instead of just below the others. Thus, in Fig. 8, the robot reaches a “steady-state” velocity close to $v_{\max} = 1.2$ m/s in the open areas.

VI. CONCLUSIONS

In this paper, we have first presented the well-known DWA to fast and safe obstacle avoidance in an unknown environment. We then recast the approach in a continuous nonlinear control framework suggested by [3]. With a few changes to the basic scheme, we were able to prove convergence to the goal position. This is significant, since the earlier scheme could be subject to limit cycles, and even divergence.

APPENDIX

LYAPUNOV STABILITY THEORY

Lyapunov theory is a very elegant and powerful tool used in stability analysis of nonlinear systems. We follow Sastry [22] closely, but for the sake of clarity and conciseness, we sacrifice some generality, e.g., time dependence.

Throughout this section, we consider a system of nonlinear differential equations

$$\dot{x} = f(x), \quad x(t_0) = x_0 \quad (12)$$

where $x, x_0 \in \mathbb{R}^n$ and $f(\cdot) : \mathbb{R}^n \rightarrow \mathbb{R}^n$. A condition to guarantee existence and uniqueness of solutions is further needed, e.g., f locally satisfying the Lipschitz condition

$$\|f(x_1) - f(x_2)\| \leq l \|x_1 - x_2\|$$

where $l \in \mathbb{R}^+$ is a fixed scalar. Points of interest in stability analysis are the so-called stationary or equilibrium points.

Definition 6.1 (Equilibrium Point)

x^* is said to be an equilibrium point of (12) if

$$f(x^*) = 0.$$

We will now go on to investigate if a given equilibrium point is stable or not.

Definition 6.2 (Stable Equilibrium)

The equilibrium point $x^* = 0$ is said to be a *stable* point of (12) if, for all $\epsilon > 0$, there exists a $\delta(\epsilon)$ such that

$$\|x_0\| < \delta(\epsilon) \Rightarrow \|x(t)\| < \epsilon \quad \forall t \geq t_0$$

where $x(t)$ is the solution of (12).

Definition 6.3 (Asymptotic Stability)

The equilibrium point $x^* = 0$ is said to be an *asymptotically stable* point of (12) if

- 1) it is stable;
- 2) it is attractive, i.e., there exists a δ such that

$$\|x_0\| < \delta \Rightarrow \lim_{t \rightarrow \infty} \|x(t)\| = 0$$

where $x(t)$ is the solution of (12).

Note that 2) above does not necessarily imply 1). Before stating the main stability result of Lyapunov theory, we need one more definition.

Definition 6.4 (Locally Positive Definite Function)

A continuous function $V(x) : \mathbb{R}^n \rightarrow \mathbb{R}^+$ is called a locally positive definite function if, for some $h > 0$ and $\alpha(\cdot)$

$$V(0) = 0 \text{ and } V(x) \geq \alpha(\|x\|) \quad \forall x : \|x\| \leq h$$

where $\alpha(\cdot) : \mathbb{R}^+ \rightarrow \mathbb{R}^+$ is continuous, strictly increasing, and $\alpha(0) = 0$.

Theorem 6.1 (Basic Lyapunov Theorem)

Suppose we are given a system (12), an equilibrium point $x^* = 0$, and a locally positive definite function $V(x)$.

- 1) If $-\dot{V} \geq 0$ (locally), then x^* is stable.
- 2) If $-\dot{V}$ is locally positive definite, then x^* is asymptotically stable.

In both cases above, we call the function $V(\cdot)$ a *Lyapunov function*.

For further results, we refer to the textbook used here [22].

REFERENCES

- [1] D. Fox, W. Burgard, and S. Thrun, "The dynamic window approach to collision avoidance," *IEEE Robot. Autom. Mag.*, vol. 4, pp. 23–33, Mar. 1997.
- [2] O. Brock and O. Khatib, "High-speed navigation using the global dynamic window approach," in *Proc. IEEE Int. Conf. Robot. Autom.*, Detroit, MI, May 1999, pp. 341–346.
- [3] J. A. Primbs, V. Nevistic, and J. C. Doyle, "Nonlinear optimal control: A control Lyapunov function and receding horizon perspective," *Asian J. Control*, vol. 1, no. 1, pp. 14–24, Mar. 1999.
- [4] E. Rimon and D. Koditschek, "Exact robot navigation using artificial potential functions," *IEEE Trans. Robot. Autom.*, vol. 8, no. 5, pp. 501–518, Oct. 1992.
- [5] P. Ögren and N. Leonard, "A provably convergent dynamic window approach to obstacle avoidance". presented at *2002 IFAC World Congr.* [CD-ROM]
- [6] —, "A tractable convergent dynamic window approach to obstacle avoidance," in *Proc. IEEE/RSJ Int. Conf. Intell. Robot. Syst.*, Lausanne, Switzerland, Oct. 2002, pp. 595–600.
- [7] C. Stachniss and W. Burgard, "An integrated approach to goal-directed obstacle avoidance under dynamic constraints for dynamic environments," in *Proc. IEEE/RSJ Int. Conf. Intell. Robot. Syst.*, Lausanne, Switzerland, Oct. 2002, pp. 508–513.
- [8] P. Althaus and H. Christensen, "Behavior coordination for navigation in office environments," in *Proc. IEEE/RSJ Int. Conf. Intell. Robot. Syst.*, Lausanne, Switzerland, Oct. 2002, pp. 2298–2304.
- [9] J. Lawton, B. Young, and R. Beard, "A decentralized approach to formation maneuvers," *IEEE Trans. Robot. Autom.*, vol. 19, no. 6, pp. 933–941, Dec. 2003.
- [10] J. Latombe, *Robot Motion Planning*. Boston, MA: Kluwer, 1991.
- [11] E. W. Dijkstra, "A note on two problems in connexion with graphs," *Numer. Math.*, vol. 1, pp. 269–271, 1959.
- [12] R. C. Arkin, *Behavior-Based Robotics*. Cambridge, MA: MIT Press, 1998.
- [13] K. O. Arras, J. Persson, R. Siegwart, and N. Tomatis, "Real-time obstacle avoidance for polygonal robots with a reduced dynamic window," in *Proc. IEEE/RSJ Int. Conf. Intell. Robot. Syst.*, Lausanne, Switzerland, Oct. 2002, pp. 3050–3055.
- [14] N. Y. Ko and R. G. Simmons, "The lane-curvature method for local obstacle avoidance," in *Proc. IEEE/RSJ Int. Conf. Intell. Robot. Syst.*, vol. 3, Vancouver, BC, Canada, Oct. 1998, pp. 1615–1621.
- [15] J. A. Benayas, J. L. Fernández, R. Sanz, and A. R. Diéguez, "The beam-curvature method: A new approach for improving local real-time obstacle avoidance". presented at *2002 IFAC 15th Int. World Congr.* [CD-ROM]
- [16] J. Minguez and L. Montano, "Robot navigation in very complex, dense and cluttered indoor/outdoor environments". presented at *2002 IFAC 15th Int. World Congr.* [CD-ROM]
- [17] O. Khatib, J. Minguez, and L. Montano, "Reactive collision avoidance for navigation with dynamic constraints," in *Proc. IEEE/RSJ Int. Conf. Intell. Robot. Syst.*, Lausanne, Switzerland, Oct. 2002, pp. 588–594.
- [18] P. Iniguez and J. Rosell, "A hierarchical and dynamic method to compute harmonic functions for constrained motion planning," in *Proc. IEEE/RSJ Int. Conf. Intell. Robot. Syst.*, vol. 3, Lausanne, Switzerland, Oct. 2002, pp. 2335–2340.
- [19] A. Elnagar and A. M. Hussein, "Motion planning using Maxwell's equations," in *Proc. IEEE/RSJ Int. Conf. Intell. Robot. Syst.*, vol. 3, Lausanne, Switzerland, Oct. 2002, pp. 2347–2352.
- [20] D. E. Chang and J. E. Marsden, Gyroscopic forces and collision avoidance. presented at *Conf. Honor of A. J. Krener's 60th Birthday*. [CD-ROM]
- [21] P. Jensfelt and S. Kristensen, "Active global localization for a mobile robot using multiple hypothesis tracking," *IEEE Trans. Robot. Autom.*, vol. 17, no. 5, pp. 748–760, Oct. 2001.
- [22] S. Sastry, *Nonlinear Systems: Analysis, Stability, and Control*. New York: Springer-Verlag, 1999.



Petter Ögren (M'04) was born in Stockholm, Sweden, in 1974. He received the M.S. degree in engineering physics and the Ph.D. degree in applied mathematics from the Royal Institute of Technology (KTH), Stockholm, Sweden, in 1998 and 2003, respectively.

In 2001, he visited the Mechanical Engineering Department, Princeton University, Princeton, NJ, for four months. He is currently working as a Researcher with the Swedish Defence Research Agency (FOI), Stockholm, Sweden. His research interests include

multirobot systems, formations, navigation, and obstacle avoidance.



Naomi Ehrich Leonard (S'90–M'95–SM'02) received the B.S.E. degree in mechanical engineering from Princeton University, Princeton, NJ, in 1985, and the M.S. and Ph.D. degrees in electrical engineering from the University of Maryland, College Park, in 1991 and 1994, respectively.

She is a Professor of Mechanical and Aerospace Engineering with Princeton University, and also an Associated Faculty Member of the Program in Applied and Computational Mathematics at Princeton. From 1985 to 1989, she worked as an Engineer in the electric power industry for MPR Associates, Inc., Alexandria, VA. Her research focuses on the dynamics and control of mechanical systems using nonlinear and geometric methods. Current interests include underwater vehicles, mobile sensor networks, and adaptive sampling with application to observing and predicting physical processes and biological dynamics in the ocean.